PRAMANA
— journal of
physics

Vol. 70, No. 3
March 2008
pp. 457–470

Numerical calculations of potential distribution in non-ideal quadrupole trap and simulations of anharmonic oscillations

ANITA GUPTA and PUSHPA M RAO*
Spectroscopy Division, Bhabha Atomic Research Centre, Mumbai 400 085, India
*Corresponding author. E-mail: pushpam@magnum.barc.ernet.in

MS received 13 July 2007; revised 13 August 2007; accepted 28 August 2007

Abstract. A quadrupole ion trap consisting of electrode structures symmetric about z-axis is an important tool for conducting several precision experiments. In practice the field inside the trap does not remain purely quadrupolar, and can be calculated using numerical methods. We have used boundary element method to calculate the potential inside the truncated as well as symmetrically misaligned quadrupolar ion trap. The calculated potential values are fitted to multipole expansion and the weights of multipole moments have been evaluated by minimizing the least square deviation. The higher-order multipole contribution in the fabricated hyperbolic electrodes due to truncation and machining imperfections is discussed. Non-linear effects arising due to the superposition of octupole moment manifest as anharmonic oscillations of trapped ions in the non-ideal Paul trap. Theoretical simulations of non-linear effects have been carried out.

Keywords. Quadrupole ion trap; multipole moments; boundary element method.

PACS Nos 32.80.Pj; 33.80.Ps; 39.10.+j; 42.50.Vk; 41.20.Cv; 02.60.Lj

1. Introduction

Ion traps have been extensively used in nuclear and atomic spectroscopy for precision measurements and more recently in quantum optics experiments with single trapped ions. For all precision measurements it is a prerequisite to obtain a near quadrupole field in the region of trapped ions resulting in a harmonic motion of trapped ions [1–3].

An ideal ion trap producing a pure quadrupole field would consist of three infinitely extended hyperbolic electrodes. Confinement of charged particles is achieved by applying AC voltage superimposed on DC potential, resulting in harmonic oscillations. The frequency of trapped ion oscillation is independent of the radial and axial oscillation amplitudes. Thus, a collection of ions with the same charge-to-mass ratio will have approximately the same frequency resulting in a narrow linewidth for the driven resonance. However, in the case of a laboratory trap the electrodes

are truncated, with holes and slits for performing spectroscopic studies and in addition inherent defects of mechanical design and misalignments are also present. This results in deviation of the electrical potential from that of a pure quadrupole one. Brown and Gabrielse [4] have carried out detailed calculations of adjustment of voltage on compensation electrodes introduced to retain pure quadrupolar nature in the Penning trap. Gabrielse [5] carried out the first theoretical calculation of electrostatic properties of compensated Penning traps.

Lunney *et al* have used the finite element method to analyze the electric field of the trap and hence to predict the dynamics of ion collection and confinement [6]. Beaty [7] has discussed the performance of ion traps with truncated electrodes producing the nearest approximation of quadrupole potential distribution. They have used boundary element method to calculate potential distribution, and obtained the mutipole moments, by expanding it in Taylor series. Franzen [8] has carried out simulation studies superimposing the multipole fields in an ion cage. Using analytical method of the variational calculus, Wang and Franzen [9] have calculated the potential distribution in complex boundaries and have developed a method to optimize the design of non-linear quadrupole ion store. Wang *et al* [10] have derived from basic principles a general condition for non-linear resonances caused by superposition of weak multipole fields. Wang and Franzen [11] have introduced a general analytical method to calculate the multipole moments in three types of ion traps with finite electrode size. Franzen [12] has discussed the influence of the multipole fields on the mass selective instability scan in non-linear ion traps. In this paper, we have calculated the potential distribution of hyperboloidal ion trap with much higher accuracy using boundary element method along with least square method described by Wang and Franzen [11]. From these calculations we have evaluated the performance of the fabricated ion traps, namely the effects due to the truncation of trap electrodes, machining imperfections and their symmetric misalignment.

The superposition of higher-order potentials will result in anharmonic ion oscillations leading to broadening and distortion of signals [4,13,14]. Brown and Gabrielse [4] have successfully tuned out anharmonicities thereby achieving unprecedented experimental precision in their studies on geonium. Subsequently, several groups [15–20] have studied in detail the occurrences of non-linear resonances in Paul traps. Sevugrajan and Menon [21] have used perturbation method to derive an analytical relationship describing the dependence of ion secular frequency on octupole and hexapole superpositions. In the present studies, we have simulated forced ion oscillation response including the octupole moment, arising due to machining imperfections in the fabricated ion traps. From these simulations the oscillation frequency shifts that are to be expected are calculated which are important especially when ions are detected by resonant excitation.

2. Method of calculation

2.1 *Calculation of potential*

Electric potential ϕ in the absence of space charge obeys the Laplace equation

$$\nabla^2\phi = 0 \tag{1}$$

and the corresponding electric field **E** is described as

$$\mathbf{E} = -\nabla\phi. \tag{2}$$

A rotationally symmetric potential distribution in spherical polar coordinates with a closed boundary can be expressed as

$$\phi(\rho,\theta) = \phi_0 \sum_{n=0}^{\infty} A_n \frac{\rho^n}{r_0^2} P_n(\cos\theta). \tag{3}$$

The coefficients A_n are dimensionless weight factors describing the potential distribution, P_n are Legendré polynomials of order n, ϕ_0 determines the strength of the potential and r_0 is the trap radius.

Ideally a pure quadrupole potential, $\phi(r,z) = \frac{\phi_0}{r_0^2}(r^2 - 2z^2)$ where $A_n = 0$ for $n \neq 2$, in eq. (3), is achieved by a system of three infinite electrodes whose surfaces are hyperboloids of rotation along z-axis. Practical constraints necessitate the truncation of the electrodes along the line perpendicular to the asymptote at a distance ρ_0 from the center, as shown in figure 1. The truncation results in finite contribution of moments other than the quadrupole moment. The potential values inside the trap due to the truncated electrode assembly have been calculated by various numerical methods, like relaxation method [5], finite element method (FEM) [6] and boundary element method (BEM) [7,11]. BEM method is better in the sense that it would involve lesser number of nodes for the same level of accuracy achievable. The numerical method adopted in this study is the boundary element method, which involves the calculation of surface charge density $\sigma(R)$ on the electrodes, from which the potential $\phi(R)$ at any point can be evaluated and is expressed as

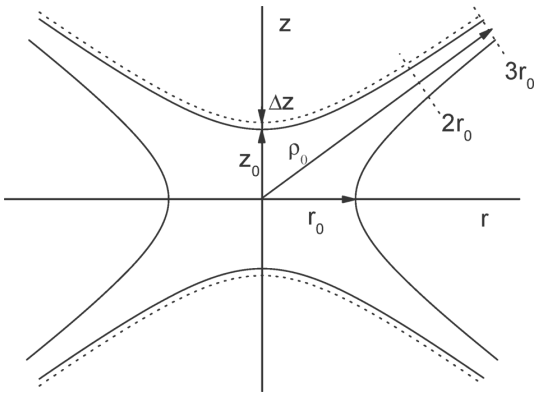

Figure 1. Ion trap comprising of hyperbolic electrodes (—) with truncations shown at $\rho_0 = 2r_0$ and $\rho_0 = 3r_0$, where r_0 is the radius of ring electrode and the distance between the two end caps is $2z_0$. Dotted line (...) shows ion trap with end caps stretched by Δz.

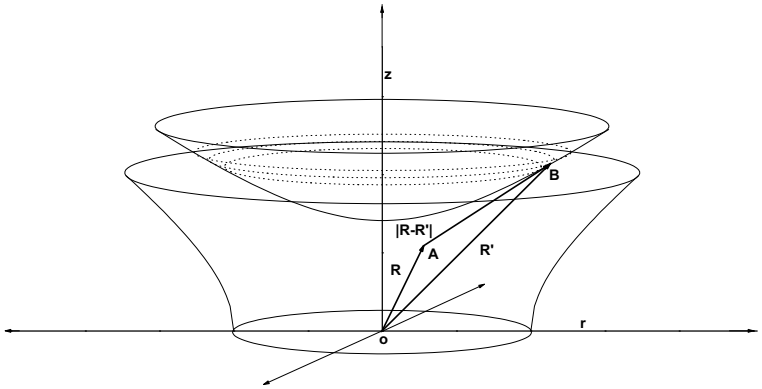

Figure 2. Figure shows a cylindrically symmetric element consisting of two cone zones. $\mathbf{R}'$ and $\mathbf{R}$ are vectors from origin to point B on the vertex of cone zones and to the point of observation A.

$$\phi(R) = \frac{1}{4\pi\varepsilon_0}\int_S \frac{\sigma(\mathbf{R}')}{|\mathbf{R}-\mathbf{R}'|}\mathrm{d}s, \tag{4}$$

where $\mathrm{d}s$ is the surface differential, $\mathbf{R}'$ and $\mathbf{R}$ are the vectors directed to the surface S and the point of observation respectively from the center, and the integration is carried out over the electrode surface S.

The procedure involves dividing the electrode surface into N cylindrically symmetric elements, each element comprising of two cone zones as shown in figure 2. Renau *et al* [22] have discussed two methods of computing surface charge density on each element; the first method involves the assumption that charge density on each element remains a constant and in the second one it varies linearly across each element. In the second method the matrix elements are more difficult to evaluate resulting in a significant increase in computational time. In the present study the magnitude of charge density on each element is assumed to be a constant and is calculated by requiring that the electrode potentials (at the vertex of cone zones) to which they give rise to be equal to the applied potential. Let us suppose that element i carries a uniform surface charge density σ_i, then the potential on element j due to charges residing on all the N elements is given as

$$\phi_j = \frac{1}{4\pi\varepsilon_0}\sum_{i=1}^{N}\sigma_i\int_S \frac{1}{|\mathbf{R}_j-\mathbf{R}_i|}\mathrm{d}s_i, \tag{5}$$

where $\mathbf{R}_i(\mathbf{R}_j)$ are vectors pointing to the vertex of cone zones of element $i(j)$. Defining the potential on the ring electrode to be $+1$ V and that on the two end caps to be -1 V, eq. (5) can be rewritten as

$$\pm 1 = \sum_{i=1}^{N} A_{ij}\sigma_i, \tag{6}$$

where the matrix element

$$A_{ij} = \frac{1}{4\pi\varepsilon_0} \int \left(\frac{1}{|\mathbf{R}_j - \mathbf{R}_i|} + \frac{1}{|\mathbf{R}_j + \mathbf{R}_i|} \right) \mathrm{d}s_i \tag{7}$$

is written only for the electrode surfaces in the region $z > 0$ as the trap electrodes possess mirror symmetry about the $z = 0$ plane, which can be expressed in terms of elliptical integral for cylindrically symmetric structure

$$A_{ij} = \frac{1}{\pi\varepsilon_0} \left(\frac{K(m)}{\sqrt{(r_j + r_i)^2 + (z_j - z_i)^2}} + \frac{K(m_1)}{\sqrt{(r_j + r_i)^2 + (z_j + z_i)^2}} \right) \int r_i \, \mathrm{d}l_i, \tag{8}$$

where $K(m)$ is the complete elliptical integral of the first kind expressed in terms of the parameter m,

$$m = \frac{4r_i r_j}{(r_j + r_i)^2 + (z_j - z_i)^2} \quad \text{and} \quad m_1 = \frac{4r_i r_j}{(r_j + r_i)^2 + (z_j + z_i)^2}.$$

If the potential is evaluated at the element i due to charge on the element itself ($i = j$), eq. (8) becomes singular. This problem is overcome by approximating the matrix element A_{ii} as

$$A_{ii} = \frac{1}{\pi\varepsilon_0} \left\{ \frac{1}{2r_i} \left[\left(\ln \frac{16r_j}{w_i} + 1 \right) - \frac{w_i^2}{576r_i^2} \left(3 \ln \frac{16r_i}{w_i} + 4 \right) \right] + \frac{K(m_1)}{2\sqrt{r_i^2 + z_i^2}} \right\} \int r_i \, \mathrm{d}l_i, \tag{9}$$

where w_i is the width of element i and the integration is carried out on the curve l_i of the corresponding element [22].

Once all matrix elements are calculated, the surface charge density can be evaluated by solving the set of linear equations (eqs. (6)), from which potential at any point in space can be determined.

2.2 *Calculation of multipole moments*

It is important to express the potential distribution in the entire region of ion oscillation in terms of spherical harmonics, as this throws light on the extent to which higher-order multipoles contribute. Beaty [7] has determined the coefficients of spherical harmonics (multipole moments) directly from the calculated surface charge density on the electrodes, by expanding the potential (eq. (5)) in Taylor series. Wang and Franzen [11] have employed the variational calculus method stating that the method described by Beaty [7] is accurate only around the center.

We have employed least square fitting to calculate multipole expansion coefficients A_n described in eq. (3). The factors A_n are determined by approximating this equation to match the potential values on a closed surface S' and minimizing

the square deviation. That is, $\sum_{S'} \int_{s_j} (\phi_j - \phi)^2 \mathrm{d}s_j$ is minimized with respect to coefficients A_n, leading to a set of linear equations,

$$\sum_{n=1}^{M} A_n \int_{S'} \left(\frac{\rho}{r_0}\right)^n P_n(\cos\theta) \left(\frac{\rho}{r_0}\right)^m P_m(\cos\theta)\mathrm{d}s = \sum_{S'} \phi_j \left(\frac{\rho}{r_0}\right)^m P_m(\cos\theta) s_j, \quad (m = 0, 2, 4, \ldots, M), \tag{10}$$

where M is the number of multipole terms to be evaluated. Because the trap electrode structure is symmetric with respect to $z = 0$ plane, odd multipole terms vanish and only the terms with even values of n have to be considered.

2.3 *Anharmonic oscillations*

Considering the first-order approximation, the leading term in eq. (3) will be the octupole component superimposed on the quadrupole field. In Paul mode of trapping the potential ϕ_0 applied between the end caps and the ring electrode is of the form $U_{\mathrm{DC}} + V_{\mathrm{AC}} \cos \Omega t$, where Ω is the frequency of the applied potential. The instantaneous potential in cylindrical coordinates is given as

$$\phi(r, z, t) = (U_{\mathrm{DC}} + V_{\mathrm{AC}} \cos \Omega t) \times \left[\frac{A_2}{r_0^2}(2z^2 - r^2) + \frac{A_4}{r_0^4}\left(4a^4 - 12z^2r^2 - \frac{3}{2}r^4\right)\right]. \tag{11}$$

In the pseudo-potential well approximation, the ion motion is depicted as composed of a small amplitude but high frequency ripple δ superimposed on a slowly varying but larger amplitude macromotion Z [23,24]. The equation of motion in this approximation is written as

$$m\ddot{Z} = -e\nabla[U_{\mathrm{DC}}\phi(r, z) + U_{\mathrm{eff}}], \tag{12}$$

where

$$U_{\mathrm{eff}} = \frac{1}{2m\Omega^2}\langle|\nabla\phi(r, z)|^2\rangle.$$

Neglecting the axial and radial couplings of the ion motion due the octupole potential, the effective potential is given as

$$U_{\mathrm{eff}} = \frac{e}{m\Omega^2}\left(\frac{V_{\mathrm{AC}}}{r_0^2}\right)^2 \left[A_2(2Z^2 + r^2) + \frac{A_4}{r_0^2}(16Z^4 - 3r^4)\right], \tag{13}$$

where $\langle\ \rangle$ means averaging over a period of $2\pi/\Omega$.

The equation of motion of the trapped ion including damping γ and under the influence of external excitation F at frequency ω_0 swept at rate b about the ion secular frequency ω_z, is given as [25]

$$m\ddot{Z} + \gamma\dot{Z} + \omega_z^2\left(Z + \frac{8}{r_0^2}\frac{A_4}{A_2}Z^3\right) = F\cos\omega_0 t, \tag{14}$$

where ω_z depends on the trapping parameters U_{DC}, V_{AC} and Ω.

To the first approximation the solution is given by [26,27]

$$Z = a\cos(\theta + \varphi), \tag{15}$$

where $\theta = \omega_0 t$ and $\omega_0 = \omega_z + bt$, b is the rate at which the external excitation frequency is swept.

Assuming that the sweep is linear and close to the ion secular frequency and that it is swept at a rate $b \ll \omega_0$, θ can be approximated to ω_0 [26,27]. The amplitude a and the phase φ are determined by the following differential equations:

$$\begin{aligned}\dot{a} &= -\frac{\gamma a}{2} - \frac{F\cos\varphi}{2(\omega_0 + \dot{\varphi})}\\ \dot{\varphi} &= \omega_z - \omega_0 + \frac{3\omega_z}{r_0^2}\frac{A_4}{A_2}a^2 + \frac{F\sin\varphi}{2a\omega_z}.\end{aligned} \tag{16}$$

In stationary mode ($b \to 0$), $\dot{a} \to 0$, $\dot{\varphi} \to 0$ the detuning $\Delta\omega$ is given by

$$\Delta\omega = \sqrt{\left(\frac{F}{2a\omega_z}\right)^2 - \left(\frac{\gamma}{2}\right)^2} - \frac{3\omega_z}{r_0^2}\frac{A_4}{A_2}a^2, \tag{17}$$

where $\Delta\omega = \omega_0 - \omega_z$. This is a cubic equation in a^2 and its real roots give the amplitude of the forced oscillations. Figure 3 shows the typical dependence of amplitude a on the excitation frequency with detuning $\Delta\omega$. It is seen from the frequency response curve that when the excitation is small the trapped ions behave as a linear system and the profile is Lorentzian. When the external excitation is large, the non-linear terms are to be included which give rise to anharmonic oscillations, resulting in the appearance of amplitude-dependent shift in ion secular frequency, exhibiting hysteresis and jump phenomena when the excitation frequency is swept around resonance.

3. Results and discussion

Citing the limitation of computer memory, Wang and Franzen [11] have divided the electrode surfaces only into 42 elements in the region $z > 0$, which is the main source of error in their calculations. In addition, for different truncation distances considered, they have divided the electrodes into the same number of elements and as a result the length of the element varies, which adds up to the error.

In the present work we have divided the electrode surface into elements of arc length 80 μm, uniformly distributed in the first quadrant, resulting in 320 and 425 elements on the ring electrode and end cap respectively for $\rho_0 = 2r_0$ truncation and for a trap of radius $r_0 = 20$ mm. Figures 4a and 4b show the surface charge density $\frac{\sigma}{\phi_0}$ C/(Vm^2) evaluated on the ring and end cap electrodes as a function of z and r respectively.

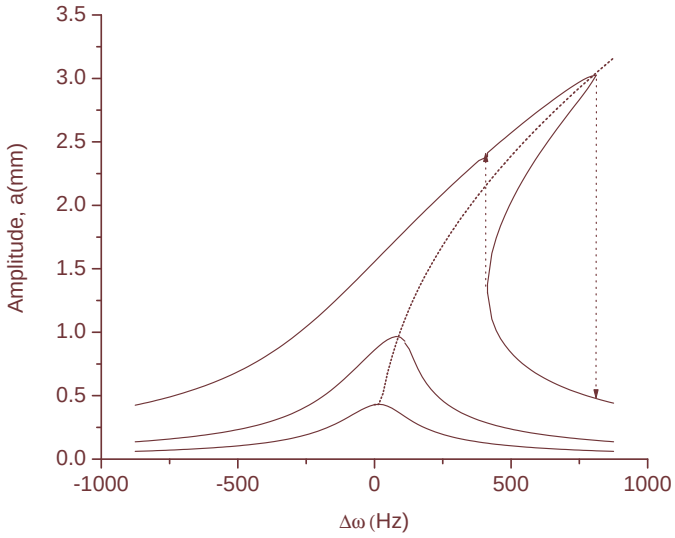

Figure 3. Plot of frequency response curve, i.e. oscillation amplitude a vs. detuning $\Delta\omega$ at three different excitations.

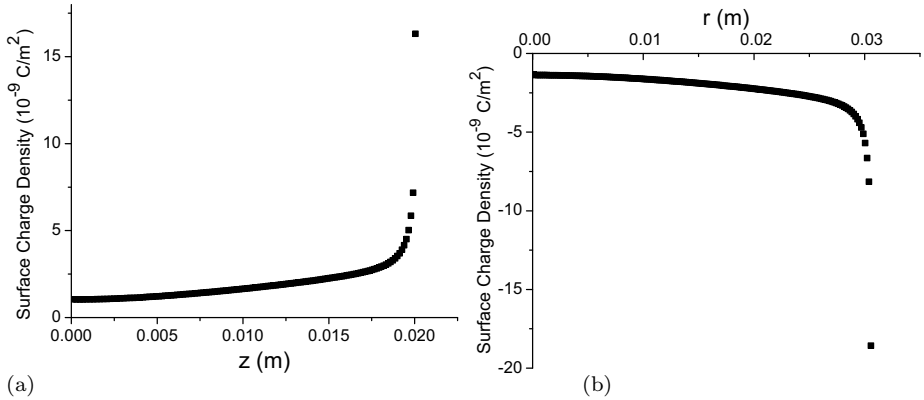

Figure 4. Surface charge densities on the (**a**) ring electrode as a function of z coordinate and (**b**) end cap electrode as a function of r coordinate.

Wang and Franzen [11] mention that the choice of closed boundary is arbitrary and for their calculations they have considered a closed surface comprising of end cap, ring electrode and the truncation line (figure 1). Their calculation suffers higher error in the estimated potentials as the point of evaluation (i.e. the truncation line) is close to the electrode surface [28]. Secondly, with this choice of boundary one has to deal with ill-conditioned matrices.

In the present work, least square fitting was performed on two different closed boundaries, a cylindrical surface (radius $r_0 - \delta$, height $2(z_0 - \delta)$) (figure 5) and a spherical surface (radius $z_0 - \delta$), both of them a few grid points away from the electrode surfaces. To evaluate the multipole moments, the least square fit has been

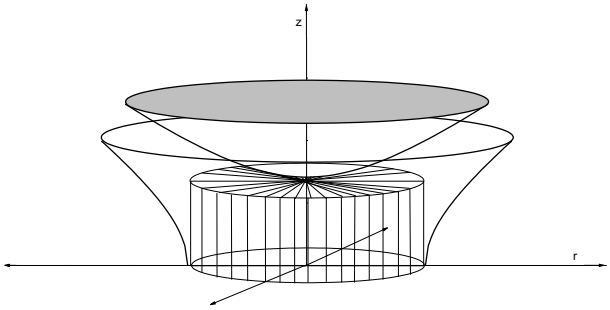

Figure 5. Closed boundary surface, comprising of a cylinder of radius $(r_0 - \delta)$ and height $(z_0 - \delta)$, constructed inside the trap electrodes.

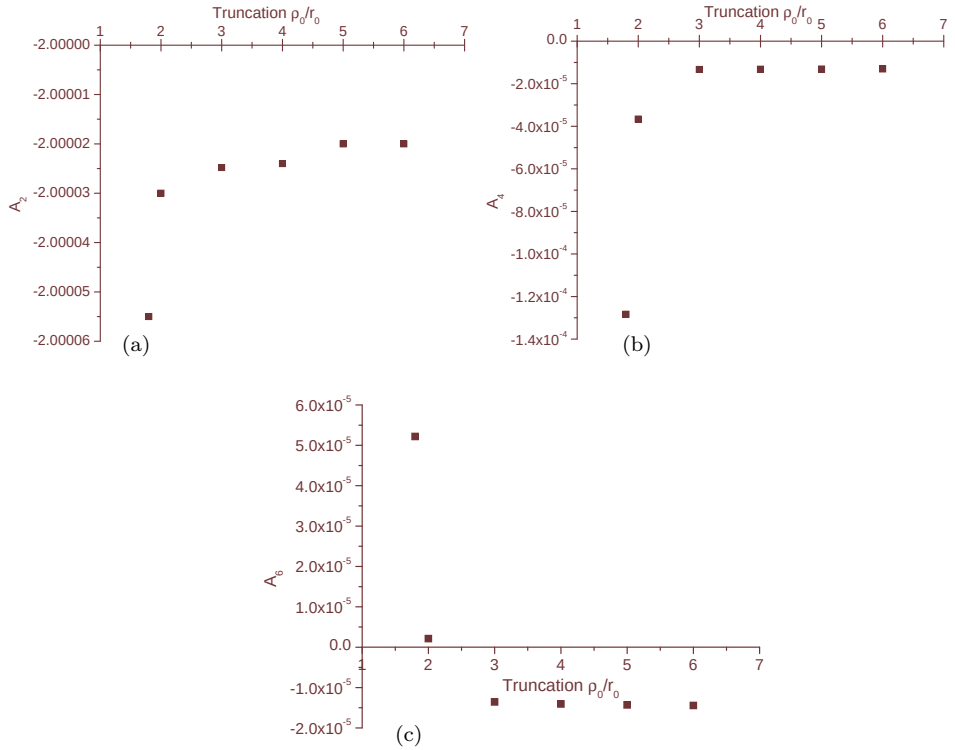

Figure 6. Variation of (**a**) quadrupole (A_2), (**b**) octupole (A_4) and (**c**) dodecapole (A_6) moments with truncation distance ρ_0.

performed for 32 multipole terms, which is adequate as further increase does not significantly change the lower-order values.

According to Wang and Franzen [11], multipole expansion represents the potential distribution in the region enclosed by the surfaces used in least square fit. We have evaluated the moments by least square fitting of the potential on z-axis (from $z = 0$ to $z_0 - \delta$) to a polynomial, which is in close agreement with our calculations

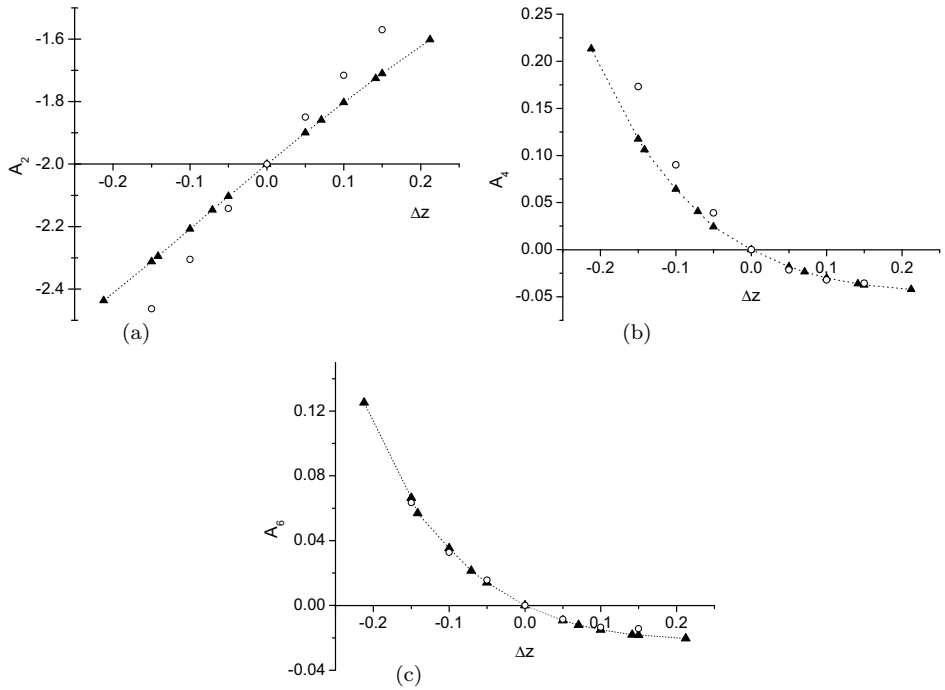

Figure 7. Variation of (**a**) quadrupole (A_2), (**b**) octupole (A_4) and (**c**) dodecapole (A_6) moments with percentage stretching, Δz. Full triangles (▲) represent our calculated values and open circles (○) represent values taken from Wang and Franzen [11].

using cylindrical and spherical surfaces (table 1). This shows that the multipole expansion evaluated even along z-axis represents the potential distribution in the whole region enclosed by the electrodes and least square fit around a closed surface for the calculation of multipole moments is not imperative.

Figures 6a–6c show the variation in quadrupole (A_2), octupole (A_4) and dodecapole (A_6) moments with truncation distance ρ_0. Our calculations show that a pure quadrupole field is obtained even if the trap electrodes are truncated at $\rho_0 = 2r_0$. And higher-order non-linear components arise mainly due to other factors, i.e. holes, slits, and one of the electrodes in the form of a mesh, or from alignment imperfections [4].

Ideally, the ratio of distance between the two end cap electrodes and the radius of ring electrode is $1/\sqrt{2}$ ensuring a pure quadrupolar field. In the present work, we have symmetrically stretched the two end caps by $2\Delta z$ as shown in figure 1.

The surfaces of the stretched end caps can be described as $z = \pm(\sqrt{(r^2 + r_0^2)/2} + \Delta z)$. Figures 7a–7c show the calculated values of quadrupole, octupole and dodecapole moments of trap truncated at $\rho_0 = 2r_0$ respectively, as a function of stretched end cap distance Δz. From our calculations it is seen that stretching the end caps symmetrically increases the non-linearity in the trap. The calculations of Wang and Franzen [11] deviate from our estimated values of moments, as the accuracy of their calculations is lower, due to the reasons stated earlier.

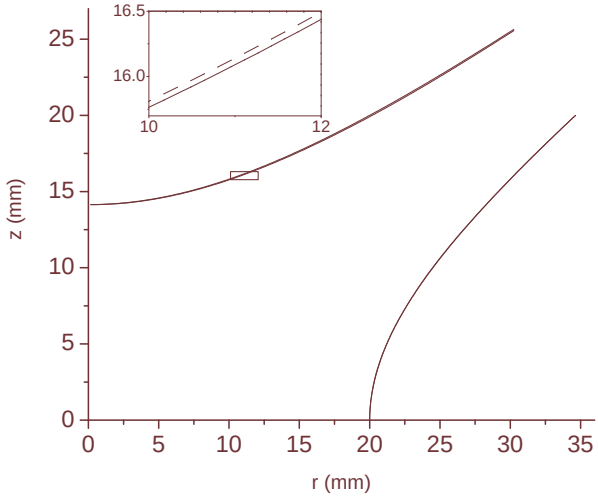

Figure 8. Truncated ion trap electrodes shown in the first quadrant. Inset shows the electrode surfaces of an ideal ion trap (—) along with the digitized profile of the fabricated trap (- - -).

Table 1. Quadrupole (A_2), octupole (A_4) and dodecapole (A_6) moments calculated by least square fit along different boundaries.

Fitted along	A_2	A_4	A_6
Cylindrical surface	-2.00005	-3.6×10^{-5}	2.1×10^{-6}
Spherical surface	-2.00004	-2.0×10^{-5}	8.2×10^{-6}
z-axis	-2.00004	-2.2×10^{-5}	12.3×10^{-6}

Ideally, the quadrupole ion trap comprises a system of three electrodes whose surfaces are hyperboloid, but machining imperfections give rise to deviation from the ideal. To estimate this deviation, the digitized surface profile of the fabricated ion trap (figure 8) has been used to calculate the higher-order moment contributions using the method described earlier and is compared with that of an ideal profile generated at the same truncation length. For numerical calculations, each electrode surface has been divided into 250 elements in the region $z > 0$. The maximum deviation of digitized profile from the ideal is ± 50 micron and the least count of digitization is 10 microns. Table 2 shows the calculated multipole moments for the fabricated trap of radius 11.3 and 20 mm and shows that the contribution of octupole (A_4) and dodecapole (A_6) moments is less than 0.13% of the quadrupole moment (A_2). From these calculations it is seen that the fabricated ion traps produce a near quadrupole field.

The error in our calculations arises due to the approximations and assumptions in the methodology adopted and due to the numerical truncation. Increasing the number of elements N improves the accuracy, as the error scales as N^{-3} [28], and is limited by the numerical truncation error. Figures 9a–9c show the values of A_2, A_4 and A_6 calculated for different element sizes (varying from 40 to 2×10^3 microns).

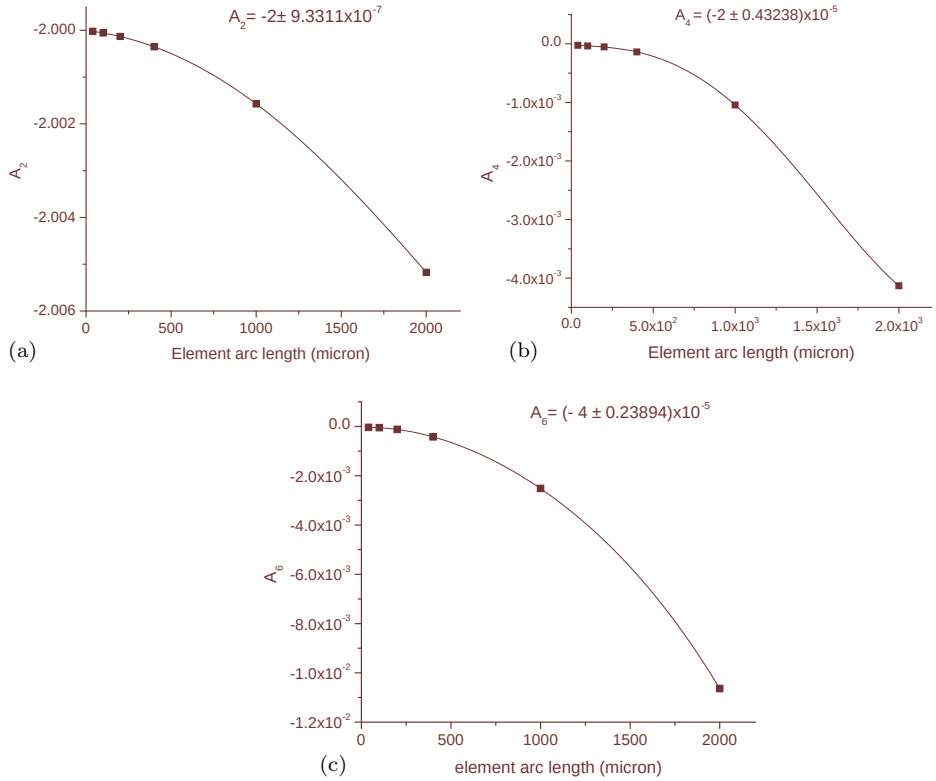

Figure 9. Variation in calculated values of (**a**) quadrupole A_2, (**b**) octupole A_4 and (**c**) dodecapole A_6 moments, with different element sizes.

In our calculations we have optimally chosen the element size of 80 microns, as the values of the calculated moments do not change with any further decrease and tends to the value extrapolated to zero element size (figures 9a–9c).

We have carried out simulations of ion response curve with A_4 values as -2.553×10^{-3} and 2.600×10^{-4}, calculated (table 2) for the fabricated ion traps with $r_0 = 20$ mm and 11.3 mm respectively. Figure 10 shows shift in ion secular frequency with varying amplitudes. The frequency shift has been shown for the positive sweep direction. From simulation of frequency response curves it is seen that the performance of the trap fabricated with $r_0 = 11.3$ mm would be superior and is more suited to study the trapped ion oscillation frequencies.

4. Conclusion

Neglecting holes, slits and asymmetric misalignments of the ion trap electrodes, the contribution of higher-order multipole moments solely due to finite truncation of electrodes has been calculated using BEM and least square fitting. For the truncated ion traps the corresponding weight factors A_n decrease with increasing

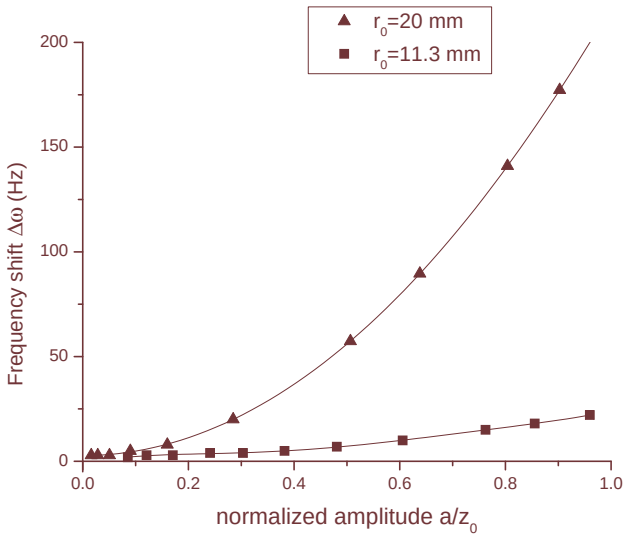

Figure 10. Plot of frequency shift ($\Delta\omega$) calculated from simulations of frequency response profiles with varying oscillation amplitudes a (mm) for fabricated trap of radius 20 mm (▲) and 11.3 mm (■).

Table 2. Comparison of quadrupole (A_2), octupole (A_4) and dodecapole (A_6) moments calculated for the ideal trap and the fabricated ion traps of radius $r_0 = 11.3$ and 20 mm.

	$r_0 = 11.3$ mm, $\rho_0 = 3r_0$ truncation		$r_0 = 20$ mm, $\rho_0 = 2r_0$ truncation	
	Ideal	Fabricated	Ideal	Fabricated
A_2	-2.0001170	-2.0004976	-2.0000698	-2.0002281
A_4	-3.819×10^{-5}	-2.600×10^{-4}	-4.336×10^{-5}	-2.553×10^{-3}
A_6	-1.552×10^{-4}	-9.297×10^{-4}	-6.399×10^{-5}	-2.162×10^{-3}

truncation distance ρ_0. The electrode surfaces can be truncated at $\rho_0 = 2r_0$ for it still preserves the essential harmonic nature of the trap. The accuracy in calculation of potential is improved by increasing the number of elements and care is taken so that the point of evaluation is not close to electrode surface. It is also seen that for the calculation of the multipole moments, the least square fit even along the z-axis yields good results. In the case of symmetric misalignment of trap electrodes, the contributions of the higher-order moments increase with increased misalignment parameter Δz. Calculated values of multipole moments differ from that given by Wang and Franzen [11] because of higher numerical error involved in their calculations. From the calculated moments of the fabricated trap with radius 20 mm, as the contributions from the higher-order moments is less than 0.13% of the quadrupole moment, it is concluded that the trap electrode assembly would generate nearly a pure quadrupole field in the region of ion confinement. In the case of the ion trap fabricated with $r_0 = 11.3$ mm, the contribution of higher-order

moments is less than 0.05% and it is also seen from the simulations of frequency response curve that its performance would be superior compared to the trap fabricated with $r_0 = 20$ mm.

Acknowledgements

We are greatly thankful to Dr S V G Menon, Chief, Theoretical Physics Division, Bhabha Atomic Research Centre, for useful discussions at various stages of this work.

References

[1] R C Thompson, *Meas. Sci. Technol.* **1**, 93 (1990)
[2] G Savard and G Werth, *Annu. Rev. Nucl. Part. Sci.* **50**, 119 (2000)
[3] G Werth, *Phys. Scr.* **36**, 149 (1987)
[4] L S Brown and G Gabrielse, *Rev. Mod. Phys.* **58**, 233 (1986)
[5] G Gabrielse, *Phys. Rev.* **A27**, 2277 (1983)
[6] M D N Lunney, J P Webb and R B Moore, *J. Appl. Phys.* **65**, 2883 (1989)
[7] E C Beaty, *Phys. Rev.* **A33**, 3645 (1986)
[8] J Franzen, *Int. J. Mass Spectrom. Ion Process.* **106**, 63 (1991)
[9] Y Wang and J Franzen, *Int. J. Mass Spectrom. Ion Process.* **112**, 167 (1992)
[10] Y Wang, J Franzen and K P Wanczek, *Int. J. Mass Spectrom. Ion Process.* **124**, 125 (1993)
[11] Y Wang and J Franzen, *Int. J. Mass Spectrom. Ion Process.* **132**, 155 (1994)
[12] J Franzen, *Int. J. Mass Spectrom. Ion Process.* **125**, 165 (1993)
[13] X Luo, X Zhu, K Gao, J Li, M Yan, L Shi and J Xu, *Appl. Phys.* **B62**, 421 (1996)
[14] A Kajita, M Kimura, S Ohtani, H Tawara and Y Saito, *J. Phys. Soc. Jpn.* **59**, 1127 (1990)
[15] R Alhiet, C Hennig, R Morgenstern, F Vedel and G Werth, *Appl. Phys.* **B61**, 277 (1995)
[16] M Vedel, J Rocher, M Knoop and F Vedel, *Appl. Phys.* **B66**, 191 (1998)
[17] R Alhiet, S Kleineidam, F Vedel, M Vedel and G Werth, *Int. J. Mass Spectrom. Ion Process.* **154**, 155 (1996)
[18] P Paasche, C Angelescu, S Ananthmurthy, D Biswas, T Valenzuela and G Werth, *Euro. Phys. J.* **D22**, 183 (2003)
[19] T Gudjons, P Seibert and G Werth, *Appl. Phys.* **B65**, 57 (1997)
[20] A Drakoudis, M Sollner and G Werth, *Int. J. Mass Spectrom.* **252**, 61 (2006)
[21] S Sevugrajan and A G Menon, *Int. J. Mass Spectrom.* **189**, 53 (1999)
[22] A Renau, F H Read and J N H Brunt, *J. Phys.* **E15**, 347 (1982)
[23] L D Landau and E M Lifshitz, *Mechanics* (Pergamon Press, Oxford, UK, 1969)
[24] R F Wuerker, H Shelton and R V Langmuir, *J. Appl. Phys.* **30**, 342 (1959)
[25] M N Gaboriaud, M Desaintfuscien and F G Major, *Int. J. Mass Spectrom. Ion Phys.* **41**, 109 (1981)
[26] Y A Mitropol'skii, *Problems of asymptotic theory of nonstationary vibrations* (Daniel Davey, New York, 1965)
[27] M A Makarov, *Anal. Chem.* **68**, 4257 (1996)
[28] H A V Hoof, *J. Phys.* **E13**, 1081 (1980)